

# Method of Railway Subgrade Diseases (defects) Inspection, based on Ground Penetrating Radar

Yaonan Li<sup>1</sup>, Hengbai Liu<sup>1</sup>, Shilei Wang<sup>1</sup>, Bo Jiang<sup>1</sup>, Szabolcs Fischer<sup>2</sup>

<sup>1</sup>Infrastructure Inspection Research Institute, China Academy of Railway Sciences Corporation Limited, Beijing, China, 100081

<sup>2</sup>Széchenyi István University, Egyetem tér 1, H-9026 Győr, Hungary  
e-mail: liyaonan@rails.cn, liuhengbai@rails.cn, wangshilei@rails.cn, pjiang@rails.cn, fischersz@sze.hu

---

*Abstract: Due to the impact of climatic and natural factors, the normal-speed railway subgrade is vulnerable to mud pumping, water accumulation, subsidence and other defects, hereafter called diseases, that frequently occur, after a period of service. It is imperative to quickly detect subgrade diseases. On the basis of studying the law of geological radar electromagnetic signal propagation along the railway subgrade, according to the results of site excavation and verification, this paper proposes a method for railway subgrade disease inspection based on ground penetrating radar. In addition, radar image features of typical subgrade diseases are clarified herein. Practical application results show that this inspection method is effective to accurately identify subgrade diseases. In particular, it is of great significance to the rapid inspection of hidden subgrade diseases. In addition, an analysis of inspection results and distribution of subgrade diseases along the line is conducive to determining the key section for treatment of subgrade diseases.*

*Keywords: ground penetrating radar; subgrade disease; denoising; radar image; subgrade inspection device*

---

## 1 Preface

The railway industry in China has undergone a rapid development. For example, the total mileage of railways in operation reached up to about 150,000 kilometers by the end of 2021 ("Statistical Bulletin on the Development of the Transportation Industry in 2021", The Ministry of Transport of China). The railway subgrade directly bears and transfers the track gravity and the dynamic load of the train, and is also affected by geological conditions, construction and other factors, so that it is vulnerable to more and more subgrade diseases year by year [1]. In fact, in-situ excavation is one of the traditional methods for discovering subgrade diseases.

Although this method is intuitive, it is inefficient and hard to be rolled out at the railway network level because it will interfere with the normal operation of trains.

As a subgrade inspection technology, ground penetrating radar technology has been developing rapidly in recent years. Many research institutions in the world have carried out various research projects and practices in this regard. In 1998, J. Hugenschmidt successfully applied geological radars to railway subgrade inspection for the first time [2]. From then on, many countries including China carried out related experiments [3-8]. For example, Szalai S, used image methods to study the deformation of ballasted railway tracks [9]. Trong Vinh Duong *et al.* conducted the physical modeling and in-depth research and analysis on the elements of mud pumping at the interface of railway ballast/subgrade, including particle distribution, water content, pore water pressure, and hydraulic conductivity [10]. Xu Xinjun studied the deep learning and target inspection of geological radar image features of mud pumping through the fast regional convolutional neural network [11]. Yang Xin'an proposed a method for identifying the development, distribution forms and diseases of mud pumping according to radar images in 2004 [12]. In 2010, Du Panfeng proposed to classify the mud pumping diseases according to geological radar waveform stacking diagram [13]. In 2015, Hou Zhezhe explored a typical subgrade disease classification method based on radar image features through the study of actual detection data and theoretical analysis [14]. Sysyn proposed a non-destructive measurement method to investigate the distribution of the ballast consolidation along the sleeper [15, 16]. Liu studied the effect of different tamping operations on the longitudinal vibration transfer characteristics of the track bed and the frequency response function of the track bed under different temperature and humidity conditions [17, 18]. PAY Ibrekk assessed the abilities of a GPR system to detect anomalies like ballast pockets and to map the distribution of water in railway ballast [19].

Thanks to these studies and applications, the role of geological radars in detecting and positioning railway subgrade diseases has been gradually accepted. However, due to the differences in the hardware equipment of geological radars, processing software and processes, there is no unified standard for identifying railway subgrade diseases through geological radars. In order to solve the aforesaid problems, this paper explores a geological radar inspection method for subgrade diseases. Through this method, the distribution state of the subgrade disease along the long trunk line can be evaluated, and the basis for the treatment of subgrade disease can be provided.

## 2 Inspection Method

### 2.1 Inspection Principle

The geological radar method is used to detect and locate the target object according to the reflection characteristics of electromagnetic waves and the change law of propagation speed of the interface between the propagation media with different dielectric constants. With high-frequency or ultra-high-frequency electromagnetic waves as the information carrier, this method has the characteristics of real-time display, as well as fast, non-destructive, continuous inspection.

Electromagnetic wave signals are emitted towards the ground through the continuous movement of the antenna. When such signals encounter a medium interface with electrical property differences (such as differences in the dielectric constant) in the process of propagation inside the object, the phenomena of reflection, transmission and refraction will occur. The larger difference in dielectric constants of the media on both sides of the medium interface indicates more electromagnetic wave energy reflected. After the electromagnetic waves to be reflected are received, by the receiving antenna, that moves synchronously with the transmitting antenna, the radar host will accurately record the two-way travel time, amplitude, phase and other motion features of the reflected electromagnetic wave. On this basis, the cross-sectional scanning images of underground media can be obtained. Underground targets can be identified through processing and interpretation of radar images (its working principle is shown in Figure 1).

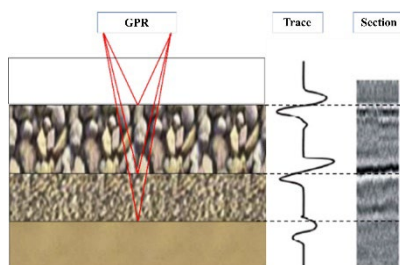


Figure 1

Schematic diagram of geological radar inspection principle

Since the propagation speed of electromagnetic waves in the same medium remains constant, the target object depth  $H$  can be calculated based on the two-way travel time  $t$  of the electromagnetic wave received and recorded. The specific calculation formula is as follows:

$$H = \frac{vt}{2} \quad (1)$$

Where,  $v = C/\sqrt{\varepsilon}$  indicates the propagation speed of electromagnetic waves in the medium,  $C$  represents the propagation speed of electromagnetic waves in the air (about  $3 \times 10^8$  m/s), and  $\varepsilon$  denotes the relative dielectric constant of the medium.

## 2.2 Inspection Device

The subgrade condition inspection system adopts IDS SRS system, which comprises a radar host, three IDS TR400 Radar antennas (corresponding to the three measurement lines distributed on the center between lines, ballast shoulders on both sides), a data acquisition instrument, a signal display instrument, a rangefinder, signal transmission cables, a global navigation satellite system(GNSS), etc. This inspection system is mounted on a special inspection vehicle, with the 25T passenger train body as the supporting platform.



Figure 2  
Subgrade inspection device

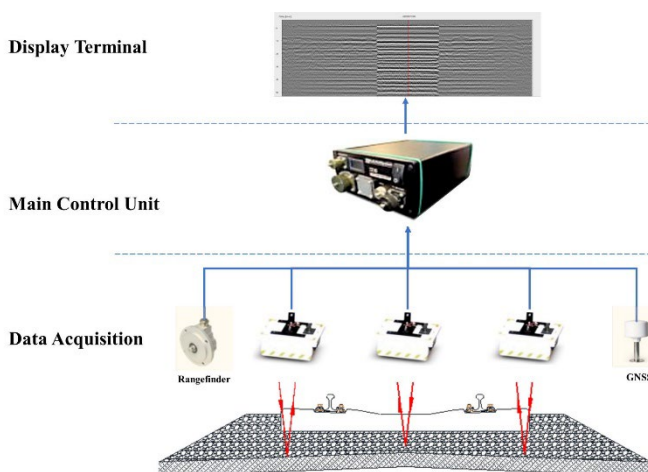


Figure 3  
Subgrade inspection system

The inspection device is shown in Figure 2, and the system composition is detailed in Figure 3. The inspection speed reaches up to 120 km/h. After the inspection system is started, the rangefinder will trigger the radar system to transmit pulse signals according to the prescribed interval. Then the data acquisition instrument will receive and record the radar wave signals reflected from the subgrade structure layer, and the display system will display the detected echo signal (namely radar image) in real time. In this way, data on each structural layer of the subgrade can be obtained.

## 2.3 Inspection Data Processing

Preprocessing of geological radar data constitutes an important part of radar data analysis. In the process of preprocessing, fidelity processing is required to ensure the reliability of subsequent analysis.

Denoising is the most important part of preprocessing. Regarding the geological radar inspection of the railway subgrade, there are two main types of noise, namely external interference noise and background noise. Specifically, external interference noise mainly includes the superimposed noise caused by the influence of signals by railway infrastructures such as Rail Sleeper, rail and catenary, as well as tunnels, bridges, slopes and other structures. In addition, background noise mainly includes the noise generated by the instruments during their operation, and also the interference noise generated in the antenna coupling process.

(1) The external interference noise is usually suppressed through the Complementary Ensemble Empirical Mode Decomposition (CEEMD) method. In 1998, the EMD method was proposed by E. Huang for the first time [20]. In 2010, the EMD method was optimized and upgraded by Yeh et al. [21] Specifically, paired auxiliary noise (positive and negative) was added to eliminate the residual auxiliary noise in the reconstructed signal, which significantly improved the computational efficiency. This new method is renamed as CEEMD. The basic principle is as follows:

Firstly, add the white noise of fixed intensity to the original signal, and decompose the additive noise signal through EMD to obtain an IMF (Intrinsic Mode Function) component; continue to decompose  $N$  kinds of white noise newly added for corresponding times, and calculate the overall average of obtained components. The specific calculation formula is as follows:

$$IMF_1 = \frac{1}{N} \sum_{i=1}^N E_i[x + \varepsilon \omega_i] \quad (3)$$

Where,  $IMF_1$  is the first-order IMF component,  $N$  represents the number of times of adding different kinds of noise,  $E_i$  indicates the  $i^{\text{th}}$  component generated by EMD decomposition,  $\varepsilon$  represents the proportion of added noise, and  $\omega_i$  denotes the added white noise. The residual generated after subtracting the first-order IMF component is calculated as follows:

$$r_1 = x - IMF_1 \quad (4)$$

Then decompose  $r_1 + \varepsilon E_1[\omega_1]$ ,  $i = 1, 2, \dots, N$ , iteratively decompose to obtain the component meeting the  $IMF_1$  conditions, and then calculate the overall average of all  $IMF_1$  to obtain the second-order  $IMF_2$  of the original signal. The specific calculation formula is as follows:

$$IMF_2 = \frac{1}{N} \sum_{i=1}^N E_i[r_1 + \varepsilon E_i[\omega_i]] \quad (5)$$

Calculate the residual of the  $k$ th order ( $r_k = r_{k-1} - IMF_k$ ), extract the first-order IMF components of  $r_k + \varepsilon E_k[\omega_1]$  ( $i = 1, 2, \dots, N$ ), and then calculate the overall

average to obtain the  $k+1$ th order component  $IMF_{k+1}$  of the original signal. The specific calculation formula is as follows:

$$IMF_{k+1} = \frac{1}{N} \sum_{i=1}^N E_i[\tau_k + \varepsilon E_k[\omega_i]] \quad (6)$$

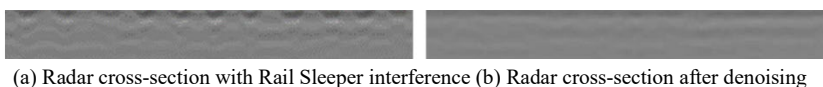
Continue to perform iterative screening until the number of extreme values of residual does not exceed 2.

$$R = x - \sum_{k=1}^K IMF_k \quad (7)$$

Where, R indicates the residual value, and K denotes the number of IMF components.

Finally, the original signal recovered from IMF component and residual sequence can be expressed as follows:

$$x = \sum_{k=1}^K IMF_k + R \quad (8)$$



(a) Radar cross-section with Rail Sleeper interference (b) Radar cross-section after denoising

Figure 4

Rail Sleeper interference removal

Figure 4 shows the effect of Rail Sleeper noise disposal. Figure 4 (a) is a radar cross-section featuring the Rail Sleeper interference, and Figure 4 (b) shows the cross-section generated after decomposition and denoising by CEEMD, with the Rail Sleeper interference removed thoroughly relatively.

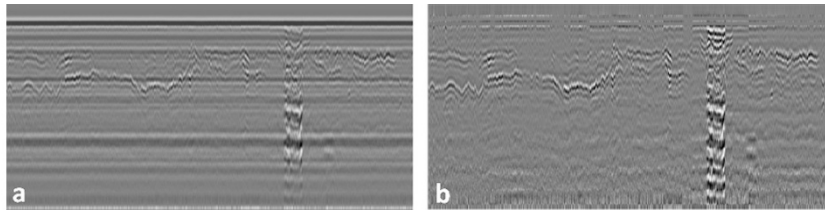
(2) The mean image denoising algorithm is used for the background noise. To enhance the regular horizontal signal and attenuate the irregular reflected signal, the mean of all track data concerning the signal segment on the radar cross-section with obvious inter-track horizontal interference is calculated. This mean can be deemed as an interference signal caused by the instrument, thus needing to be removed from all data channels of the radar cross-section. Also, this mean is regarded as the value of instrument background noise. The background noise can be eliminated by calculating the difference between background noise and all channels of radar cross-section.

The background noise is selected as follows:

$$x_z(t) = \frac{1}{N_2 - N_1 + 1} \sum_{i=N_1}^{N_2} x_i(t) \quad N_1 < N_2 \quad (9)$$

Where,  $N_1$  is the starting channel of the cross-section background noise, and  $N_2$  represents the ending channel of the cross-section background noise.

Figure 5 shows the effect of background noise disposal. Figure 5(a) is the radar cross-section with background noise, and Figure 5(b) shows the cross-section after mean background denoising. The background noise is removed thoroughly relatively, but valid signals are maintained.



a) Radar cross-section with background noise (b) Radar cross-section after denoising

Figure 5

Background noise removal

### 3 Radar Image Features of Typical Subgrade Diseases

After data preprocessing, the signal-to-noise ratio (SNR) of geological radar inspection will be improved, and disease signal features will be clearly reflected. In combination with theoretical analysis and site excavation and verification, geological radar signal features of three subgrade diseases (namely mud pumping, water accumulation and subsidence) were analyzed and determined during the study.

(1) The radar image of mud pumping is characterized by continuous flat or undulating strong reflection coaxial axis in the depth range from the ballast bed surface to the subgrade bed surface. Differences in water containing conditions might result in the differences in multiple reflections, and cover the signals reflected from the interfaces of ballast bed and subgrade bed. What's worse, the illusion that the interface of ballast bed and subgrade bed uplifts towards the shallow layer might occur. The distance between the top surface of mud pumping and the top surface of the Rail Sleeper is limited to 25 cm. Mud pumping is further divided into concealed mud pumping (surface depth is less than 25 cm) and exposed mud pumping (surface depth is greater than 25 cm).

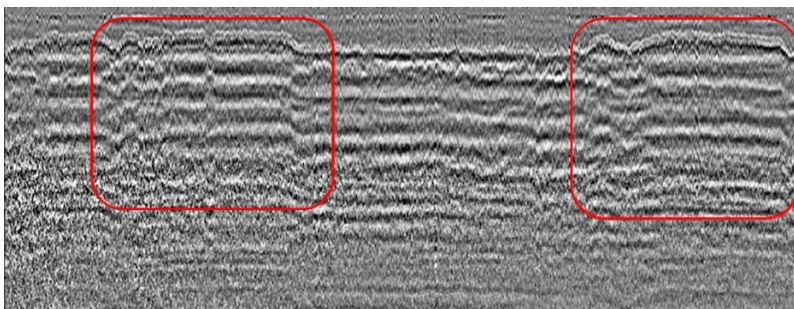


Figure 6

Radar image features of mud pumping

(2) The high water content of the subgrade or foundation might lead to the subgrade quality deterioration and instability, and further cause diseases such as mud pumping and subsidence. The image features of water accumulation are characterized by low frequency strong reflection, large amplitude, reverse phase and multiple reflections at the interface, and the interface is relatively flat.

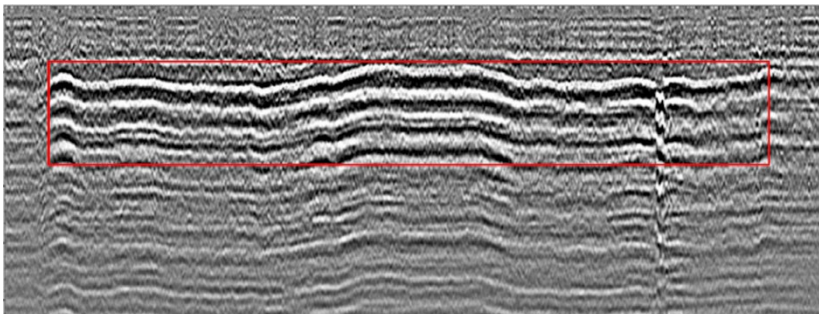


Figure 7  
Radar image features of water accumulation along the line

Subsidence refers to the local or relatively large vertical settlement or subsidence deformation under the coupling effect of water, overlying load, self-weight, climate change, dynamic train load and vibration resulting from insufficient compactness of the ballast bed, subgrade, or foundation. It is also called ballast pit, ballast sack or ballast pocket in case of local or small range with the ballast trapped in the subgrade bed. Radar image features of subsidence area as follows: The reflective events of the interface between the ballast bed and the subgrade bed structure, and between the subgrade bed surface and the substratum indicate significant bending, discontinuity or offset of the depth downwards. By the length limit of 10 m, the subsidence diseases are further divided into ballast trap (with a length of less than 10 m) and structural interface fluctuation (with a length of greater than 10 m). The subsidence is identified mainly through one-off inspection, which represents the condition of subgrade at the time of inspection. In contrast, multiple inspections are required for judging the subsequent development trend of subsidence.

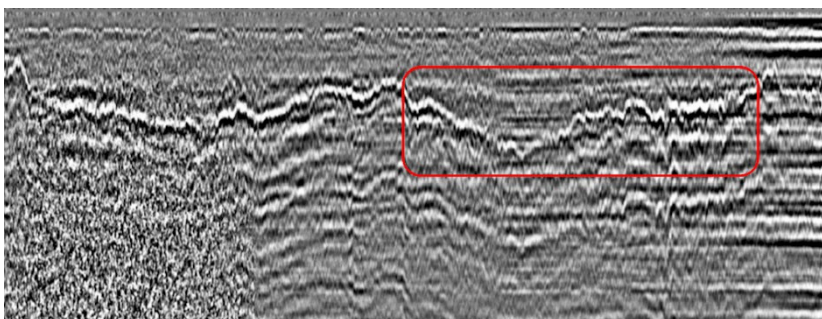


Figure 8  
Radar image features of subsidence



## 4 Case Analysis

The subgrade of a normal-speed railway in Southwest China is vulnerable to relatively serious diseases. Particularly in the rainy season, mud pumping, water accumulation, subsidence and other diseases occur frequently, and it is difficult to maintain the track geometry. In July 2021, the authors of this paper conducted site inspection of the entire railway line using the subgrade inspection method and special inspection device introduced herein. Meanwhile, the work of data processing and interpretation was carried out.

### 4.1 Summary of Inspection Results

Through inspection, diseases were found in 262 places with a cumulative length of 30,244 m, accounting for 4.50% of the total length (700 km) of subgrade inspected.

Specifically, mud pumping disease was discovered in 36 places with a cumulative length of 5,238 m, accounting for 0.78% of the total length above; water accumulation was found in 217 places with a cumulative length of 22,382 m, accounting for 3.33% of the total length; and subsidence was found in 9 places with a cumulative length of 2,624 m, accounting for 0.39% of the total length.

The distribution and proportions of various subgrade diseases are shown in Fig. 9. Specifically, by the ratio between cumulative length and total length, mud pumping, water accumulation and subsidence accounted 17.32%, 74.00%, and 8.68%, respectively.

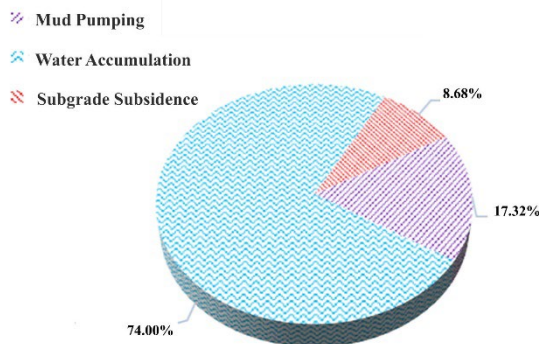


Figure 9  
Distribution of subgrade diseases

Statistical analysis was made based on the cumulative length of diseases in the 10 km interval. The results show that the cumulative length of subgrade diseases in the K1230-K1240 segment accounted for 19.70% of the total subgrade length of this segment.

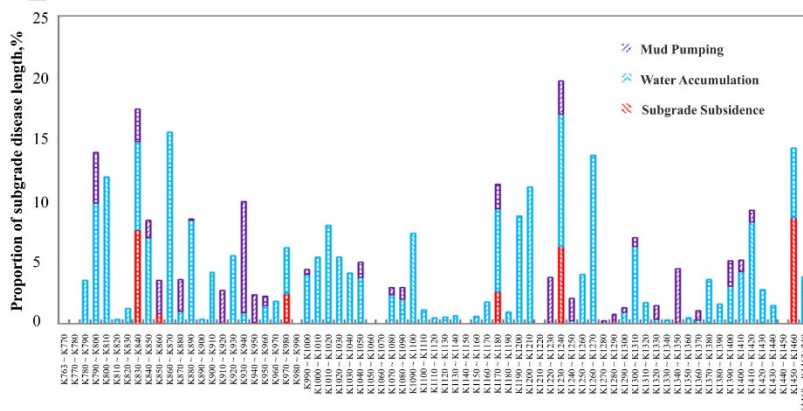


Figure 10  
Distribution of diseases along the route

Analysis of inspection data makes it possible to understand the distribution of three typical diseases by line length (Figure 10) and depth. In particular, it is useful for accurately judging whether mud pumping has occurred inside the ballast bed. In addition, the railway maintenance unit can optimize the ballast bed screening plan according to the distribution of diseases by depth. In order to ensure the long-term effect of ballast bed screening, the key subgrade diseases can be treated together.

## 4.2 Site Excavation and Verification

To verify the accuracy of inspection through this method, site excavation of 17 sections of subgrade disease development was performed. The results of geological radar recognition are relatively consistent with the in-situ excavation conditions.

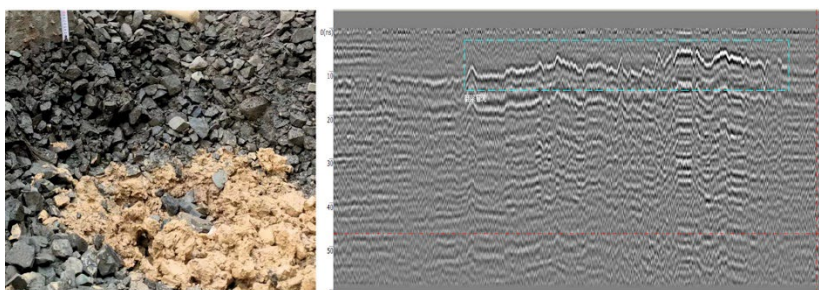


Figure 11  
Excavation and verification results of mud pumping disease along the K920+800 line

Figure 11 shows the excavation and verification results of mud pumping disease along the K920+800 line. Radar reflection waveform shows the characteristics of uneven reflections, there are multiple reflections in the underlying layer, and the

mud pumping interface has not reached the surface layer. Therefore, it is deemed as concealed mud pumping. Site excavation findings are consistent with the inspection conclusions. Obvious mud pumping was seen after excavation without access to the rail surface.

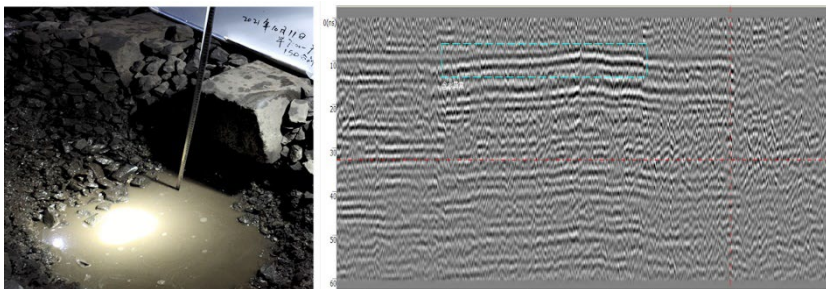


Figure 12

The result of water accumulation test of K1253+400 line

Figure 12 shows the excavation and verification results of water accumulation along the K1253+400 line. The radar reflection waveform in Figure 12 shows parallel strong reflection characteristics, and there are multiple reflections in the underlying layer. Therefore, the line is deemed as water accumulation. Site excavation findings are consistent with the inspection conclusions, and obvious water accumulation was seen after excavation.

## Conclusions

This paper proposes a method for railway subgrade disease inspection based on the geological radar. Firstly, radar data were denoised to improve the SNR, and then radar image features of typical subgrade diseases were determined according to the results of site excavation and verification. A special detection device equipment was used for rapid acquisition of geological radar data of subgrade, and effective identification of typical subgrade diseases according to comparison results of radar image features. The subgrade inspection method has been applied to a normal-speed railway in Southwest China. It is demonstrated that this method is effective to realize the rapid inspection and accurate identification of concealed subgrade defects. Conclusions are made as follows:

- (1) The CEEMD method and the mean background denoising algorithm are effective to remove the Rail Sleeper interference and background noise in the radar data, and to improve the SNR of inspection data.
- (2) This paper analyzes and summarizes the radar image features of three typical subgrade diseases, namely mud pumping, water accumulation and subsidence. According to the characteristics of typical subgrade diseases, radar inspection data of subgrade are interpreted, which provides a basis for the identification of concealed subgrade diseases.

- (3) This inspection method makes it possible to understand the distribution of three typical subgrade diseases by line length and depth, so as to support the treatment of such diseases. In particular, it is useful for accurately judging whether diseases have existed inside the ballast bed. In addition, it is conducive to optimizing the ballast bed screening plan, and ensuring the long-term effect of ballast bed screening.

### Acknowledgement

This research was funded by the Research and Development Project of China Academy of Railway Sciences Corporation Ltd., under Grant Number [2021JJXM22]: Automatic identification technology of mud pumping disease based on ground penetrating radar.

### References

- [1] National Railway Administration of People's Republic of China, "TB/T 2818-2016 Railway Roadbed Disease Classification," 2017
- [2] Hugenschmidt J, "Railway Track Inspection Using GPR," *Journal of Applied Geophysics*, Vol. 43, pp. 147-155, 2000
- [3] Clark M R, Gillespie R, Kem PT, et al., "Electromagnetic properties of railway ballast," *NDT & E International*, Vol. 34, No. 5, pp. 305-311, 2001
- [4] Sussmann T R, Selig E T, Hysli PJ P, "Railway track condition indicators from ground penetrating radar," *NDT & E International*, Vol. 36, No. 3, pp. 157-167, 2013
- [5] Geraads S, Charachon B, Loeffler O, et al. , "Applying a wavenumber notch filter to remove interferences caused by railway Rail Sleepers from a GPR section," *Ninth International Conference on Ground Penetrating Radar. Bellingham, WA : Society of Photo-Optical Instrumentation Engineers*, pp. 715-718, 2002
- [6] Wang S, Liu G, Jing G, et al., "State-of-the-Art Review of Ground Penetrating Radar (GPR) Applications for Railway Ballast Inspection," *Sensors*, Vol. 22, No. 7, pp. 24-50, 2022
- [7] Y. Guo, V. Markine, G. Jing\*, "Review of ballast track tamping: mechanism, challenges and solutions," *Construction and Building Materials*, 2021
- [8] Juhász E, Fischer S, "Tutorial on the fragmentation of the railway ballast particles and calibration methods in discrete element modelling," *Acta Technica Jaurinensis*. Vol. 14, No. 1, pp. 104-122, 2021
- [9] Szalai S, Eller B, Juhász E, et al. , "Investigation of deformations of ballasted railway track during collapse using the Digital Image Correlation Method (DICM)," *Reports in Mechanical Engineering*, Vol. 3, No. 1, pp. 258-282, 2022

- 
- [10] Trong Vinh Duong, Yu-Jun Cui, et al., "Investigating the mud pumping and interlayer creation phenomena in railway sub-structure," *Engineering Geology*, 2014
- [11] Xinjun Xu, Yang Lei, et al., "Railway Subgrade Defect Automatic Recognition Method Based on Improved Faster R-CNN," *Scientific Programming*, 2018
- [12] Yang Xinan, Gao Yanling, "Ground Penetrating Radar Detection of Slurry Flooring Diseases on Shanghai-Nanjing Railway," *Rock Mechanics and Engineering Journal*, Vol. 23, No. 1, pp. 116-119, 2004
- [13] DU Panfeng, LIAO Lijian, YANG Xin'an, "Intelligent Recognition of Defects in Railway Subgrade," *Journal of the China Railway Society*, Vol. 32, No. 3, pp. 142-146, 2010
- [14] HOU Zhezhe. "Research on GPR Images Recognition for Subgrade Defects in Ballasted Railroad," *Beijing Jiaotong University*, 2016
- [15] Sysyn, Mykola, et al. "Experimental study of railway ballast consolidation inhomogeneity under vibration loading." *Pollack Periodica* Vol. 15, No. 1, pp. 27-36, 2020
- [16] Sysyn, Mykola, et al. "Laboratory evaluation of railway ballast consolidation by the non-destructive testing." *Communications-Scientific letters of the University of Zilina* Vol. 21, No. 2, pp. 81-88, 2019
- [17] Liu, Jianxing, et al. "Influence of a tamping operation on the vibrational characteristics and resistance-evolution law of a ballast bed." *Construction and Building Materials* 239, 117879, 2020
- [18] Liu, Jianxing, et al. "Dynamic characteristics of the railway ballast bed under water-rich and low-temperature environments." *Engineering Structures* 252 .113605, 2022
- [19] PAY Ibrenk. Detecting anomalies and water distribution in railway ballast using GPR [D] Norwegian University of Science and Technology, 2015
- [20] Norden E. Huang, Zheng Shen, et al., "The Empirical Mode Decomposition and the Hilbert Spectrum for Nonlinear and Non-Stationary Time Series Analysis," *Proceedings: Mathematical, Physical and Engineering Sciences* . 1998 (1971)
- [21] Yeh, Jia-Rong, Jiann-Shing Shieh, et al., "Complementary ensemble empirical mode decomposition: A novel noise enhanced data analysis method," *Advances in Adaptive Data Analysis* Vol. 2, No. 2, pp. 135-156, 2010